# Supporting Information

## Evolutionary Mutations Reshape the Spike Protein's Conformational Landscape by Modulating Glycan Dynamics

*Wentao XU, Tianyu GUO, and Haibin SU**

*Department of Chemistry, Laboratory of Theoretical and Computational Chemistry, The Hong Kong University of Science and Technology, Hong Kong, China*

## Supporting figures

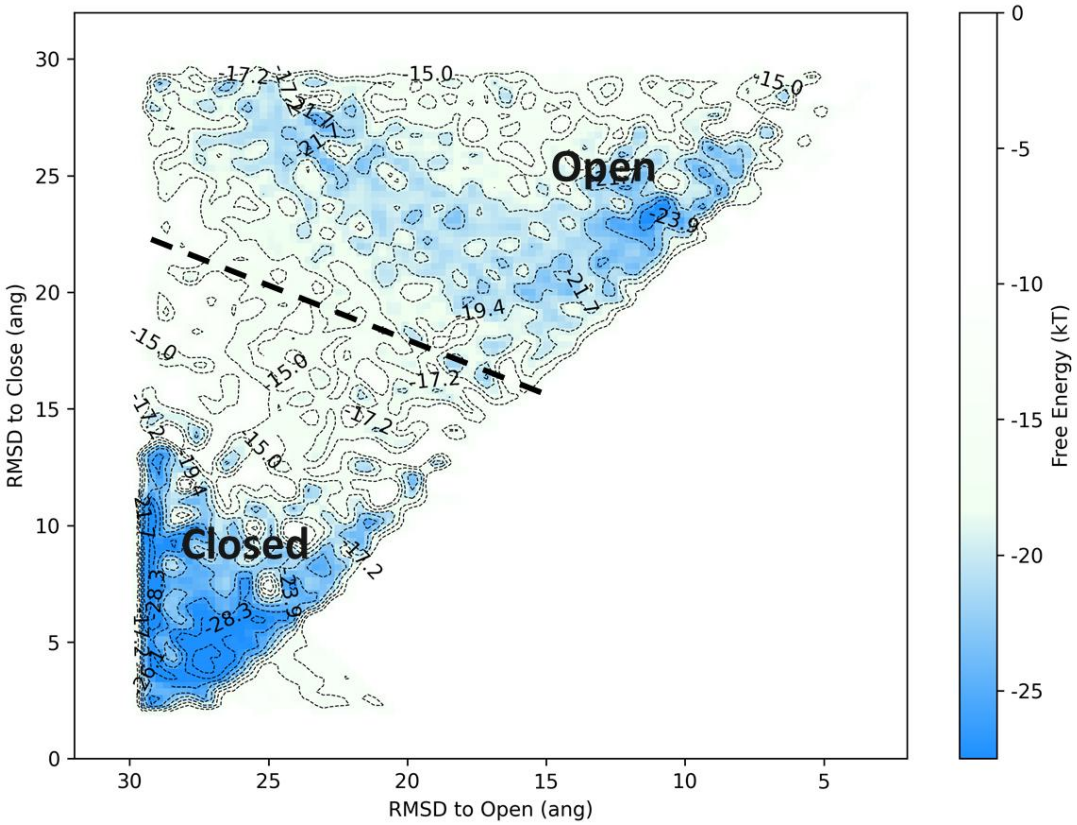


**Figure S1.** Classification and explanation of conformational states on the RMSD-based Free Energy Landscape. The figure displays a representative Free Energy Landscape (FEL) for the wild-type (WT) strain, constructed using the root-mean-square deviation (RMSD) to a reference "closed" state (x-axis) and a reference "open" state (y-axis) as collective variables. Conformational regions are demarcated by dashed lines: the "Closed" state and the "Open". This classification provides a standardized framework for the quantitative comparison of thermodynamic stability and conformational flexibility across different variants presented in **Figure** 1 and 2.

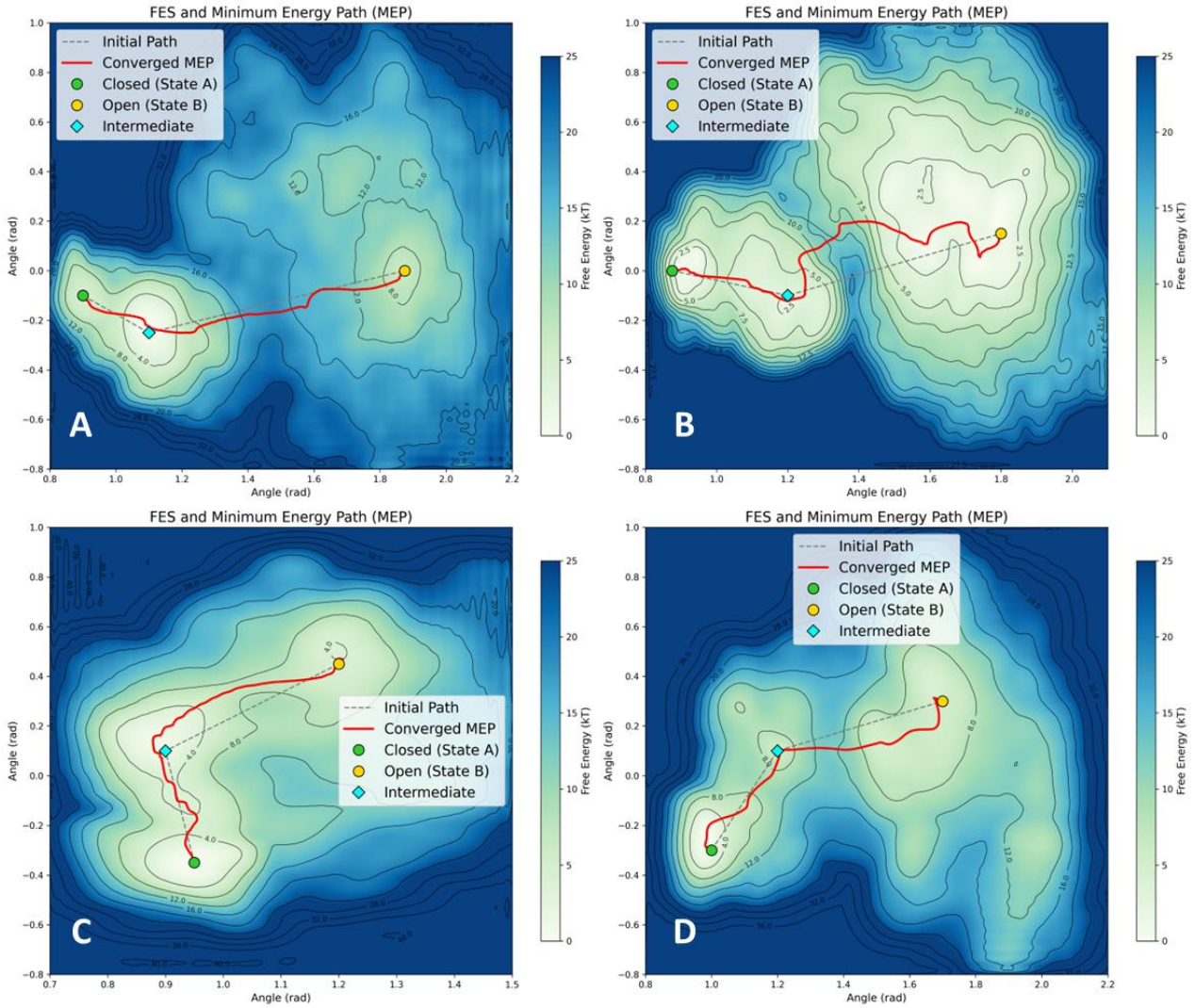


**Figure S2.** Minimum Energy Paths (MEPs) for the RBD opening transition in SARS-CoV-2 variants. The MEPs are calculated on the 2D geometric FELs for (A) Wild-Type (WT), (B) Delta, (C) BA.2, and (D) BA.4/5. In each panel, the initial path for the string method calculation is shown as a dashed grey line, while the final, converged MEP is depicted by the solid red line. The path connects the stable closed state (State A, green circle) and the open state (State B, yellow circle), passing through an intermediate waypoint (cyan diamond). The distinct topographies of the FELs and the varied trajectories of the MEPs highlight the unique kinetic pathways and energy barriers associated with the RBD opening mechanism for each variant.

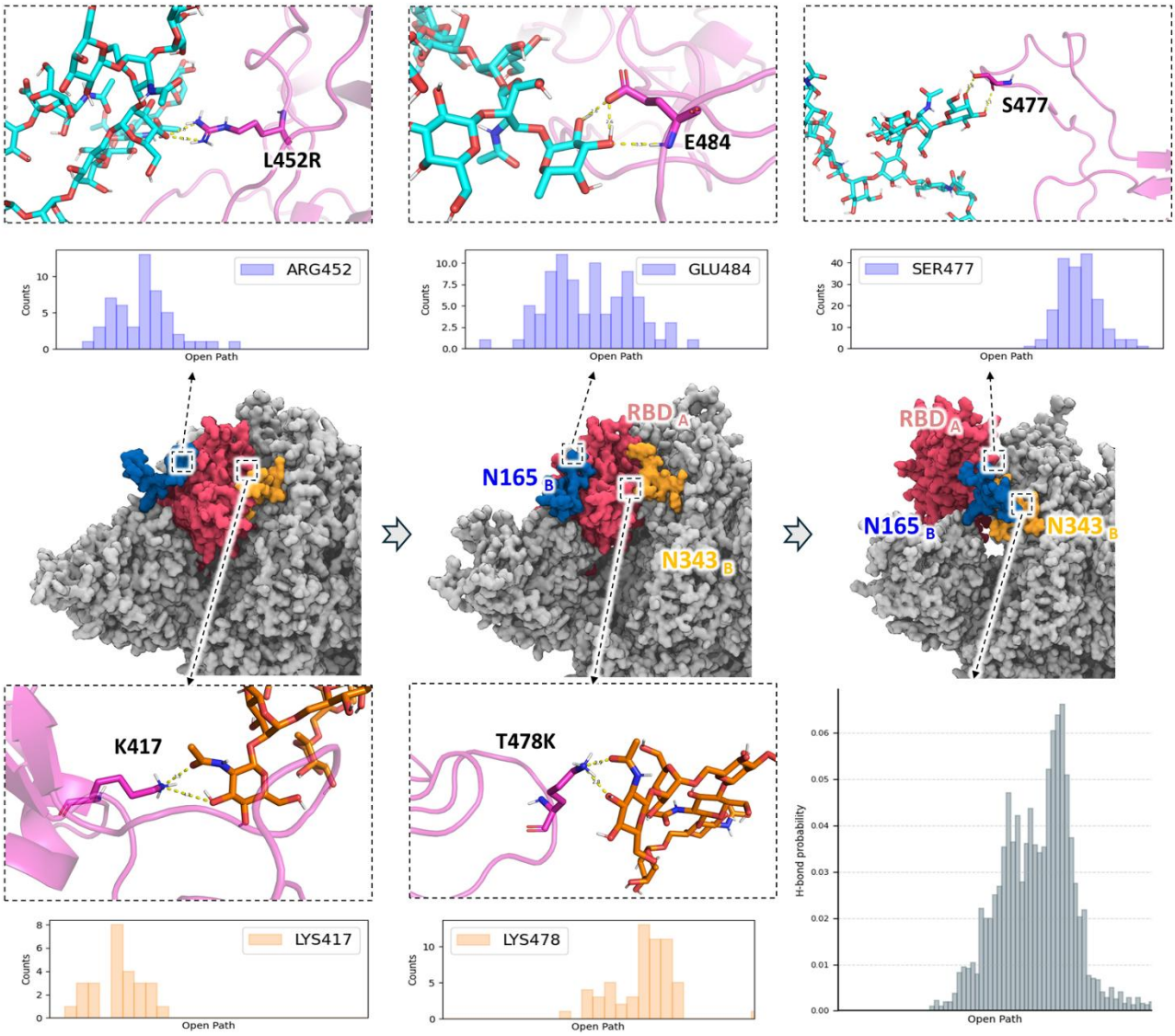


**Figure S3.** The dynamic changes in the interactions between key residues (such as L452R, E484, etc.) and adjacent glycan (N165, N343) during the transition path of the RBD of the **Delta variant** from the closed state to the open state. The lower right corner shows the mutual contact frequency between Glycan N165 and Glycan N343.

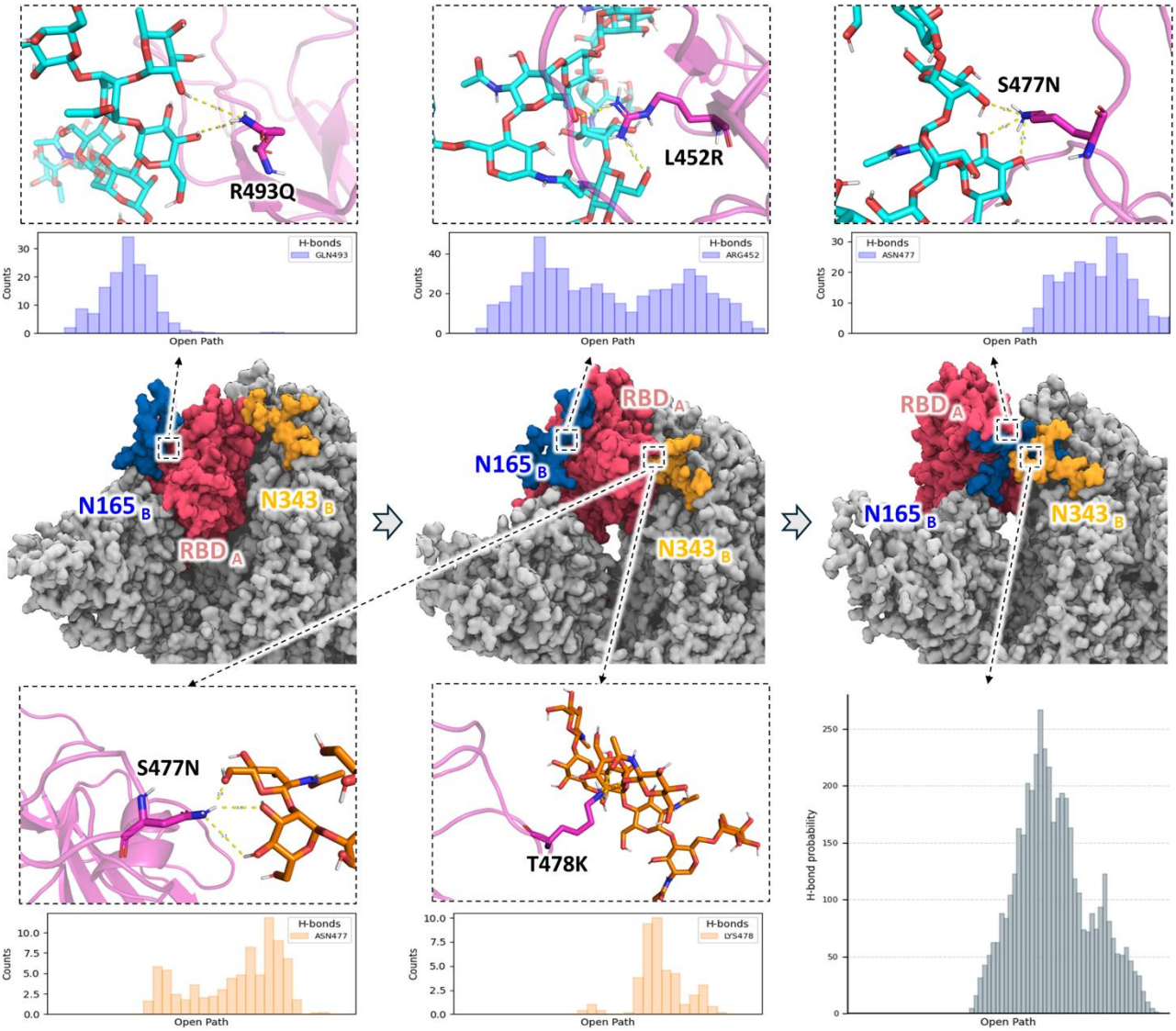


**Figure S4.** The dynamic changes in the interactions between key residues (such as L452R, E484, etc.) and adjacent glycan (N165, N343) during the transition path of the RBD of the **BA.4&5 variant** from the closed state to the open state. The lower right corner shows the mutual contact frequency between Glycan N165 and Glycan N343.

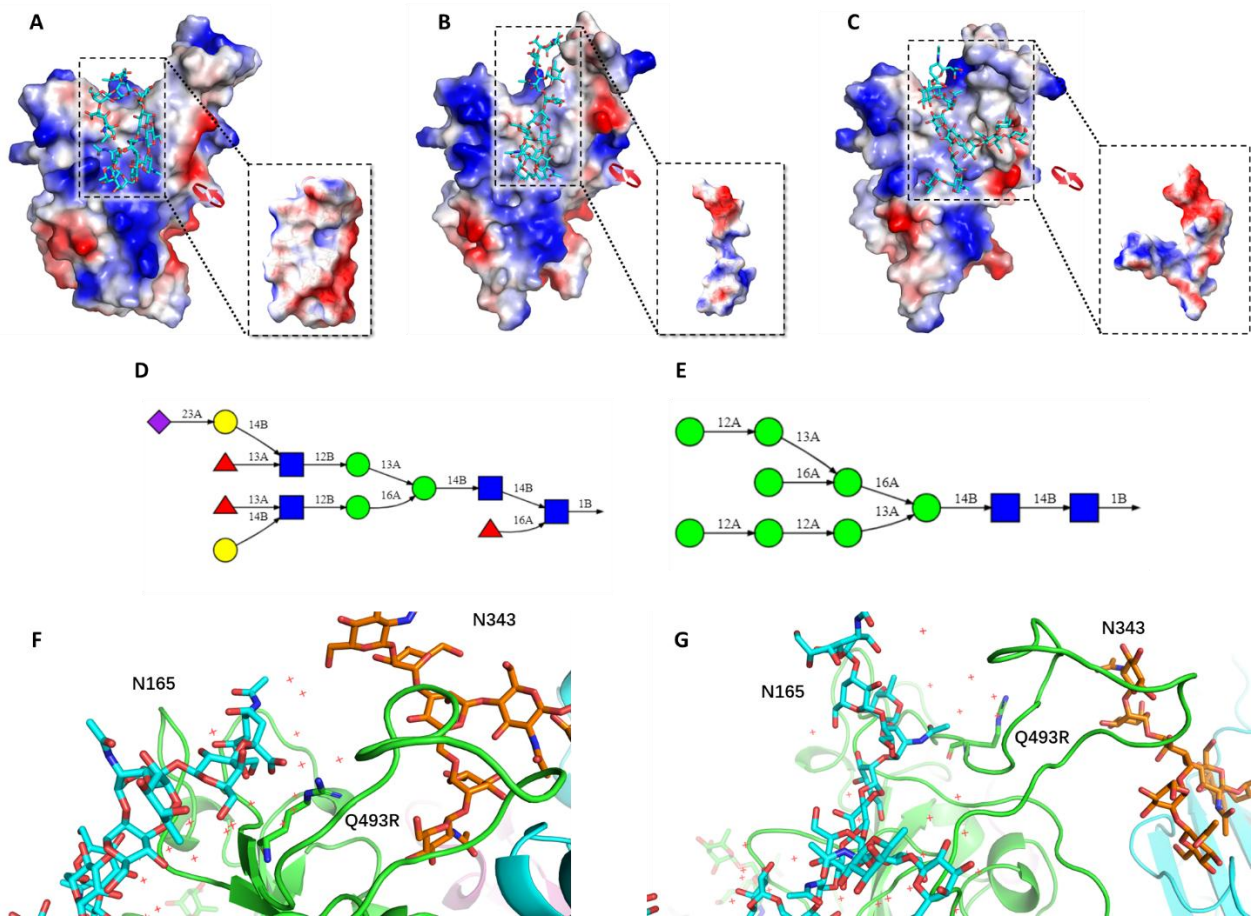


**Figure S5.** Electrostatic Complementarity and Distributed Negative Charge of the N165-Glycan. (A-C) Representative snapshots from the BA.2 variant simulation illustrating the electrostatic complementarity between the Receptor-Binding Domain (RBD) surface and the N165-glycan. The main panels show the electrostatic potential of the RBD (blue: positive, red: negative), with the complex-type N165-glycan shown in stick representation. The inset panels display the corresponding electrostatic potential surface of the isolated glycan, highlighting its overall negative charge distribution. (D) SNFG (Symbol Nomenclature for Glycans) representation of the sialylated complex-type glycan (FA2G2S1) used in the primary simulations shown in (A-C). (E) SNFG representation of the oligomannose-type glycan (Man5) used in comparative validation simulations to test the robustness of the proposed mechanism. Crucially, the analysis reveals that a significant partial negative charge is distributed across the entire glycan body, not exclusively localized to the terminal sialic acid (purple diamond in D). (F-G) The potential structural water involved in the protein-glycan interaction as shown in subfigure B and C.

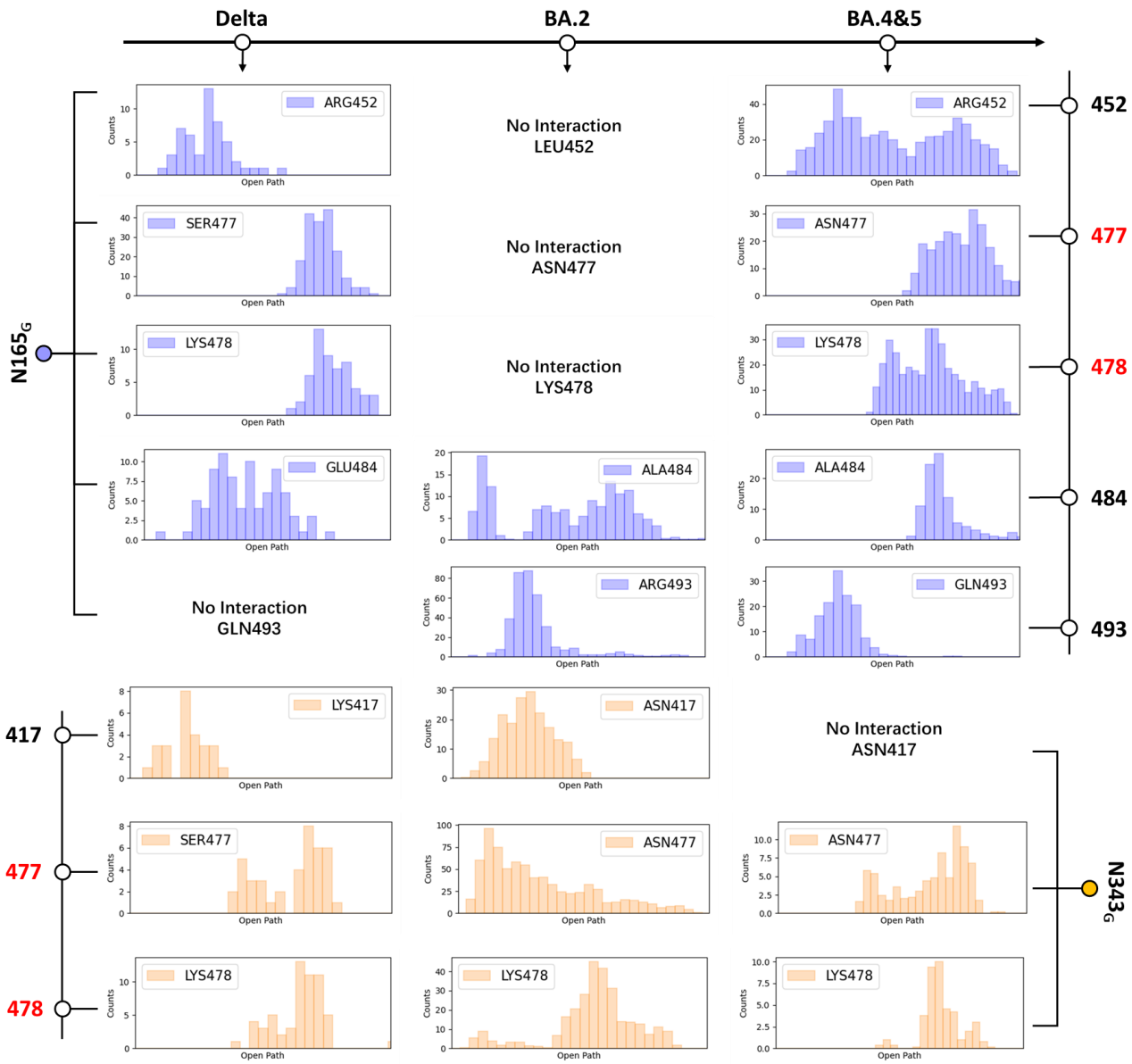


**Figure S6.** Quantitative analysis of dynamic contact between key mutations and glycans. This figure presents the contact frequencies of key mutation residues with N165 glycan (upper group in the figure) and N343 glycan (lower group in the figure) as the RBD opens along the transition path in the Delta, BA.2, and BA.4/5 variants through a histogram.

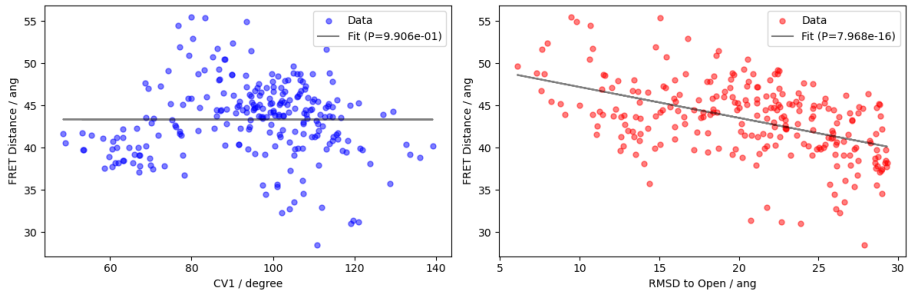


**Figure S7.** The scatter plot of the correlation between CVs and FRET distance. The left panel shows CV1, RBD open angle, with FRET distance. The right panel shows RMSD to the open value with FRET distance.

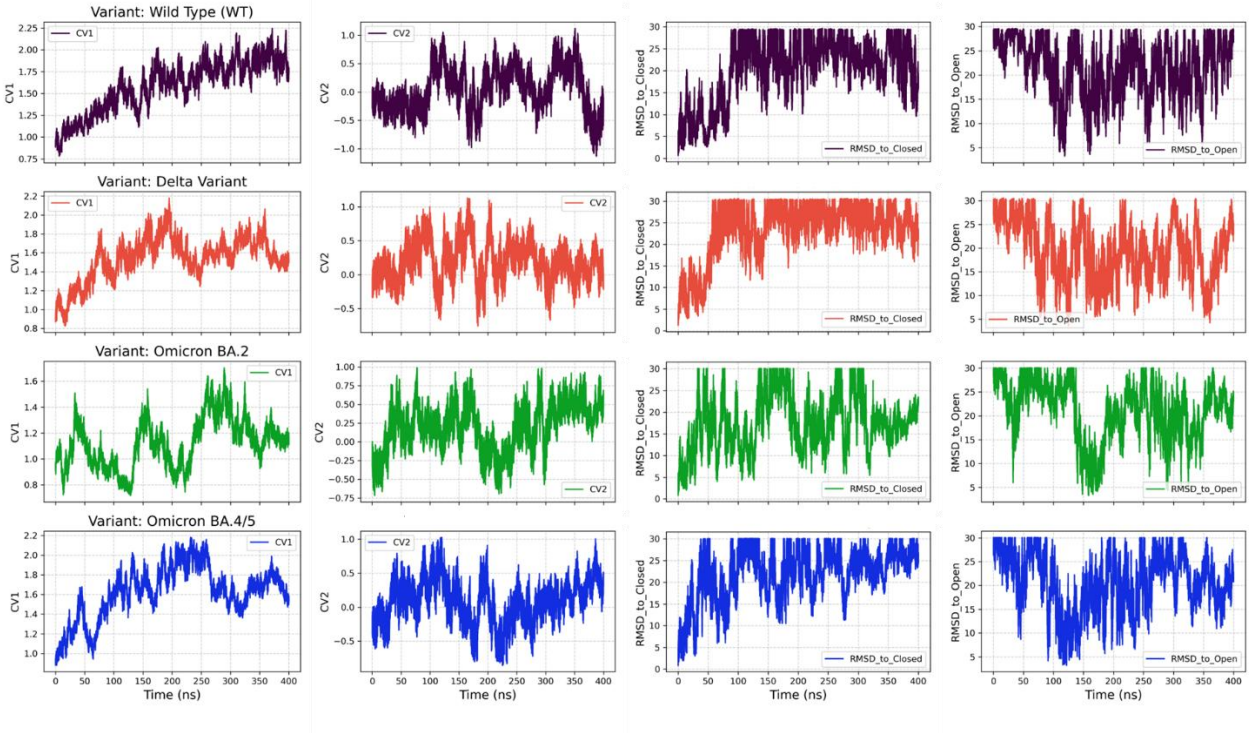


**Figure S8.** The changes in four CVs over time.

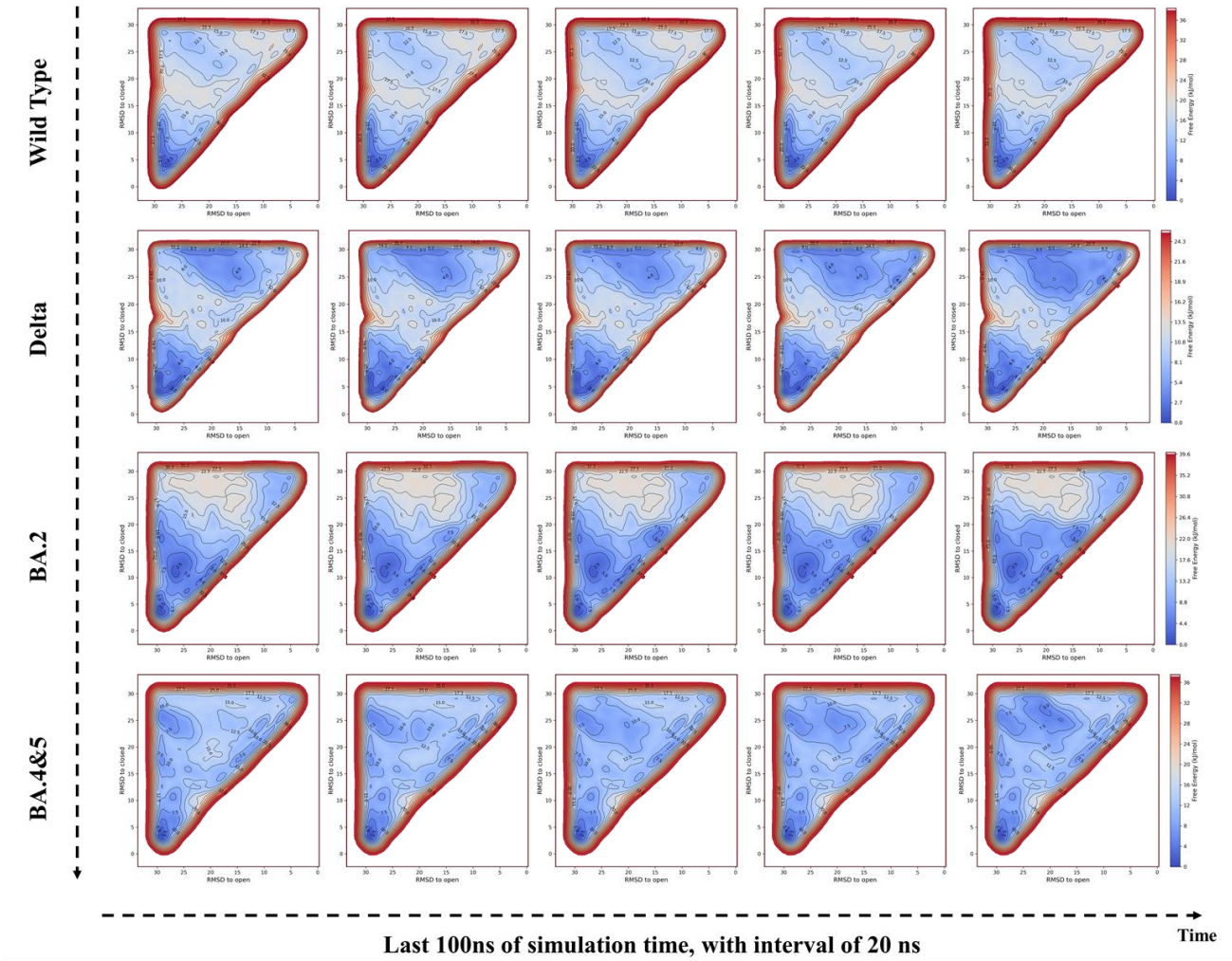


**Figure S9.** The changes in the conformational kinetic free energy of the spike proteins of various virus variants within the last 100 nanoseconds.

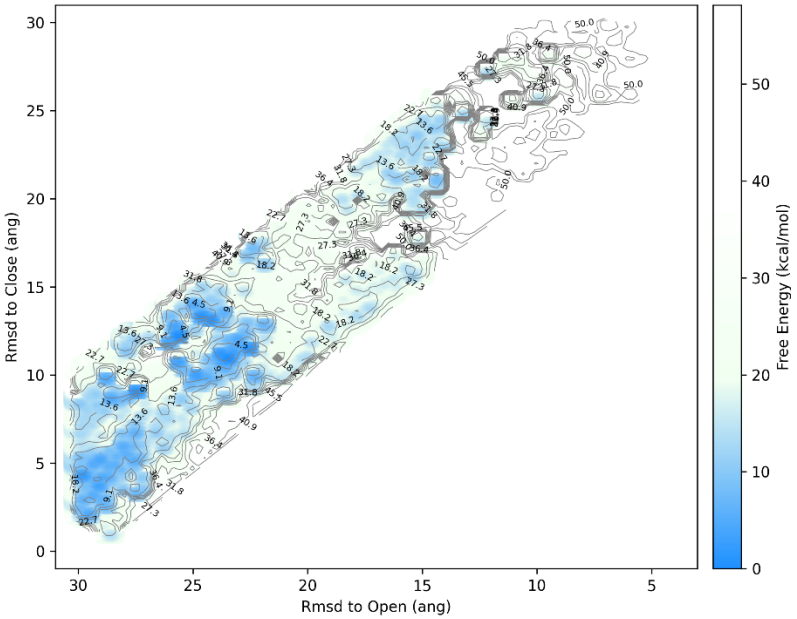


**Figure S10.** RMSD-based FEL of oligomannose-N165 glycan containing BA.2 spike protein.